A controller for stable grasping and desired finger shaping without contact sensing

M. Grammatikopoulou, E. Psomopoulou, L. Droukas and Z. Doulgeri,
Department of Electrical and Computer Engineering,
Aristotle University of Thessaloniki,
54124 Thessaloniki, Greece
e-mail: margramm@auth.gr , efipsom@ee.auth.gr , ldroukas@auth.gr , doulgeri@eng.auth.gr

***Abstract*— This paper proposes a controller for the stable grasp of an arbitrary-shaped object on the horizontal plane by two robotic fingers with rigid hemispherical fingertips. The controller stabilizes the grasp with optimal force angles and desired finger shaping determined through the choice of a control constant without requiring the utilization of any contact information regarding contact locations and contact angles or any estimates of them. Simulation results demonstrate the performance of the proposed controller and show its clear advantages with respect to other known control schemes.**

I. INTRODUCTION

A number of review papers summarizing progress on multi-finger robot grasping and dexterous object manipulation has been published in the last decade [1]–[4] showing the difficult path towards achieving the dexterity and performance of the human hand with robots. Despite building multi-fingered robot hands resembling the human hand since the early robotics research years [5]–[9] stable grasping and in-hand fine manipulation in uncertain and dynamic environments is far from being accomplished in a simple natural way.

Previous research work focuses on detailed grasp analysis and planning of form and force closure grasps [10] involving the accurate planning of fixed contact locations and contact forces [3], [4], [11], [12] later allowing contact motion via rolling and/or sliding and finger-gaiting [13]–[15] thus increasing planning and control complexity. Most of the proposed fine manipulation controllers have been hybrid position-force controllers or impedance controllers which assume fixed relative contacts (no rolling or sliding) and knowledge of the system dynamics as they essentially cancel it out as well as other precise information on the hand and object [3], [4].

A notable exception has been research work addressing the design of simple feedback control laws that attain stable grasping in a dynamic sense [16], [17] as well as object orientation, eliminating the need of precise grasp planning by allowing rolling contacts and avoiding the solution of inverse kinematics and dynamics. The superposition principle introduced in [18] and the stability on a manifold for dexterous object grasping and manipulation [19] revealed the possibility to address the control design of stable grasping, object orientation and position, independently. Enhancements in various directions followed, achieving grasping and fine manipulation blindly without force and contact sensing for objects with flat surfaces and arbitrary shape for both the 2D and 3D cases [20]–[23]. This class of controllers allows initial finger-object contact with contact locations and contact force values that do not correspond to an equilibrium state which is attained dynamically by the rolling of the fingertips. A recent work belonging also in this class of controllers concerns tactile-based grasping control of arbitrary-shaped objects focusing on grasp quality with respect to the contact force angle optimization [24]. Use of tactile sensing has been advocated for measuring exact contact locations [25] or contact angles [24] but the proposed control solutions have not been analyzed or tested with respect to their robustness on measurement errors.

In all the above research works, finger shaping or finger configuration is not considered. However, finger shaping, as grasp preshapes [26], may be important in order to best adapt to the particular geometry and subsequent intended task. In this work, we propose a dual finger control law which stabilizes the grasp of an arbitrary-shaped object in 2D with optimal force angles and desired relative finger shaping with respect to their distal links, without requiring any tactile or force sensing.

II. SYSTEM DESCRIPTION

Consider the x-y planar case of two 3 degrees of freedom robotic fingers with revolute joints and rigid hemispherical tips of radius $r_1 = r_2 = r$ in contact with a rigid arbitrary shaped object, as depicted in Fig. 1. Vector $\mathbf{q_i} = \begin{bmatrix} q_{i1} & q_{i2} & q_{i3} \end{bmatrix}^T$, $i = 1, 2$ denotes the joint angles for the i_{th} finger. In the following, R_{ab} denotes the rotation matrix of frame $\{b\}$ with reference to frame $\{a\}$ unless the reference frame is the inertia frame $\{P\}$ in which case it is omitted. $R(\theta)$ is a rotation through an angle θ about the z axis that is normal to the x-y plane pointing outwards.

Let $\{P\}$ be the inertia frame attached at the base of the first finger (Fig. 1) and $\{O\}$ be the object frame placed at its center of mass (Fig. 2) and described by the position vector $\mathbf{p_o} \in \mathbb{R}^2$ and the rotation matrix $R_o = R(\theta_o)$.

This research is co-financed by the EU-ESF and Greek national funds through the operational program "Education and Lifelong Learning" of the National Strategic Reference Framework (NSRF) - Research Funding Program ARISTEIA I

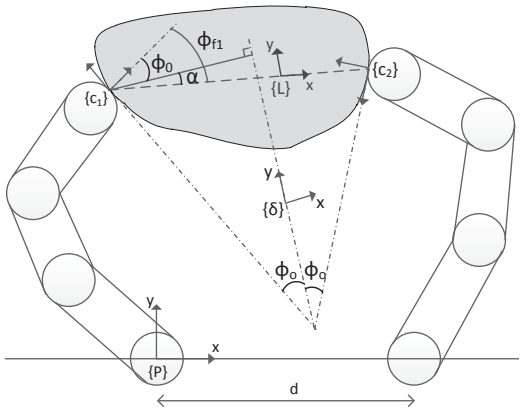

Fig. 1: Pair of robotic fingers grasping a rigid arbitrary shaped object

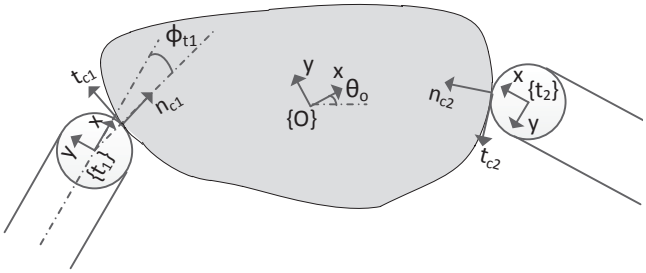

Fig. 2: Object and finger tip frames

Let $\{t_i\}$ be the i_{th} fingertip frame described by position vector $\mathbf{p_{t_i}} \in \mathbb{R}^2$ and rotation matrix $R_{t_i} = R(\phi_i)$, with $\phi_i = \sum_{j=1}^{3} q_{ij}$. Let frame $\{c_i\}$ be attached at the contact point of each finger with the object with its x axis aligned with the normal to the object surface pointing inwards. Let the orientation of $\{c_i\}$ relative to $\{t_i\}$ be described by $R_{t_1c_1} = R(\phi_{t_i})$ (Fig. 2). Frame $\{c_i\}$ is described by position vector $\mathbf{p_{c_i}} \in \mathbb{R}^2$ and rotation matrix $R_{c_i} = R(\phi_i + \phi_{t_i})$. Let $\mathbf{n_{c_i}}, \mathbf{t_{c_i}} \in \mathbb{R}^2$ be the normal pointing inwards and the tangential vectors to the object at the contact points, expressed in $\{P\}$, hence $R_{c_i} = [\mathbf{n_{c_i}}\ \mathbf{t_{c_i}}]$. Notice that $\mathbf{p_{c_i}} = \mathbf{p_{t_i}} + r\mathbf{n_{c_i}}$.

Let the two tangential lines at the contact points form an angle equal to $2\phi_0$ and $\{\delta\}$ be a frame with its y axis placed upon the bisector of the angle $2\phi_0$ at a position that can be freely chosen (Fig. 1). Line c_1c_2 is the contact interaction line with length $\|\mathbf{p_{c_2}} - \mathbf{p_{c_1}}\| = l$ generally changing with the contact location for an arbitrary shaped object. Let $\{L\}$ be a frame with its x axis placed upon the interaction line c_1c_2. The orientation of $\{L\}$ relative to $\{\delta\}$ is described by $R_{\delta L} = R(\alpha)$ (Fig. 1). From the problem's geometry it is clear that $R_{c_1\delta} = R(\phi_0)$, $R_{c_2\delta} = R(-\phi_0 - \pi)$. Combining the above $R_{c_1L} = Rot(\phi_{f_1})$ and $R_{c_2L} = Rot(\phi_{f_2} - \pi)$ where

$$\phi_{f_1} = \alpha + \phi_0,\ \phi_{f_2} = \alpha - \phi_0 \tag{1}$$

denote the angles between the interaction line and the normals to the contacts (Fig. 1) which for a value of ϕ_0 are minimized at $\alpha = 0$; the grasp controller should ideally achieve this minimum as discussed in [24]. Calculating the relative orientation of the contact frames $R_{c_1c_2}$ via the object $R_{c_1\delta}{R_{c_2\delta}}^T$ and the fingers ${R_{c_1}}^T R_{c_2}$, angles ϕ_0, ϕ_i, ϕ_{t_i} are related as follows:

$$2\phi_0 + \pi = \phi_2 - \phi_1 + \phi_{t_2} - \phi_{t_1} \tag{2}$$

We model the system under the following contact and rolling constraints [20]:

$$\begin{bmatrix} D_{ii} & D_{i3} \end{bmatrix} \begin{bmatrix} \dot{\mathbf{q}}_\mathbf{i} \\ \dot{\mathbf{p}}_\mathbf{o} \\ \dot{\theta}_o \end{bmatrix} = 0,\ \begin{bmatrix} A_{ii} & A_{i3} \end{bmatrix} \begin{bmatrix} \dot{\mathbf{q}}_\mathbf{i} \\ \dot{\mathbf{p}}_\mathbf{o} \\ \dot{\theta}_o \end{bmatrix} = 0 \tag{3}$$

where

$$D_{ii} = {\mathbf{n_{c_i}}}^T J_{v_i}, \qquad D_{i3} = \begin{bmatrix} -{\mathbf{n_{c_i}}}^T & {\mathbf{n_{c_i}}}^T \hat{p}_{oc_i} \end{bmatrix} \tag{4}$$

$$A_{ii} = {\mathbf{t_{c_i}}}^T J_{v_i} + r_i J_{\omega_i}, \quad A_{i3} = \begin{bmatrix} -{\mathbf{t_{c_i}}}^T & {\mathbf{t_{c_i}}}^T \hat{p}_{oc_i} \end{bmatrix} \tag{5}$$

with $\mathbf{p_{oc_i}} = \mathbf{p_{c_i}} - \mathbf{p_o}$ and for a vector $\mathbf{p} = [a\ b]^T$ we define $\hat{\mathbf{p}} = [b\ -a]^T$ so that $\hat{\mathbf{p}}^T\mathbf{k}\ \forall k \in \mathbb{R}^2$ defines the outer product $\mathbf{p} \times \mathbf{k}$. The Jacobian matrices $J_{v_i} = J_{v_i}(\mathbf{q_i}) \in \mathbb{R}^{2\times 3}$, $J_{\omega_i} = J_{\omega_i}(\mathbf{q_i}) \in \mathbb{R}^{1\times 3}$ relate the joint velocity $\dot{\mathbf{q}}_\mathbf{i} \in \mathbb{R}^3$ with the i_{th} fingertip linear and rotational velocities $\dot{\mathbf{p}}_{\mathbf{t_i}} \in \mathbb{R}^2$ and $\omega_{\mathbf{t_i}} = \dot{\phi}_i \in \mathbb{R}$ respectively as follows:

$$\dot{\mathbf{p}}_{\mathbf{t_i}} = J_{v_i}\dot{\mathbf{q}}_\mathbf{i}\ \ ,\ \ \omega_{\mathbf{t_i}} = J_{\omega_i}\dot{\mathbf{q}}_\mathbf{i} \tag{6}$$

The system dynamics under the contact and rolling constraints (3) on the horizontal plane is described by the following equations for both fingers and the object:

$$M_i(\mathbf{q_i})\ddot{\mathbf{q}}_\mathbf{i} + C_i(\mathbf{q_i}, \dot{\mathbf{q}}_\mathbf{i})\dot{\mathbf{q}}_\mathbf{i} + {D_{ii}}^T f_i + {A_{ii}}^T \lambda_i = \mathbf{u_i} \tag{7}$$

$$M \begin{bmatrix} \ddot{\mathbf{p}}_\mathbf{o} \\ \ddot{\theta}_o \end{bmatrix} + {D_{13}}^T f_1 + {D_{23}}^T f_2 + {A_{13}}^T \lambda_1 + {A_{23}}^T \lambda_2 = 0 \tag{8}$$

where $M_i(\mathbf{q_i}) \in \mathbb{R}^{3\times 3}, M = diag\,(M_o, I_o)$, with $M_o = diag\,(m_o, m_o)$ the positive definite inertia matrices of the i_{th} finger and object respectively and m_o, I_o denote the object's mass and moment of inertia and $C_i(\mathbf{q_i}, \dot{\mathbf{q}}_\mathbf{i})\dot{\mathbf{q}}_\mathbf{i} \in \mathbb{R}^3$ the vector of Coriolis and centripetal forces of the i_{th} finger. The Lagrange multipliers f_i and λ_i represent the applied normal and tangential constraint forces respectively at the contacts and let f_{c_i} denote the resultant contact force magnitude. Last, $\mathbf{u_i} \in \mathbb{R}^3$ is the vector of applied joint torques to the i_{th} finger.

III. PROPOSED CONTROLLER

We propose the following grasping controller:

$$\mathbf{u_i} = -k_{v_i}\dot{\mathbf{q}}_\mathbf{i} - (-1)^i\, f_d\, {J_{v_i}}^T \frac{\mathbf{p_{t_2}} - \mathbf{p_{t_1}}}{\|\mathbf{p_{t_2}} - \mathbf{p_{t_1}}\|} - (-1)^i\, r f_d\, \sin\phi {J_{\omega_i}}^T \tag{9}$$

where

$$\phi = \phi_2 - \phi_1 - \gamma_s, \tag{10}$$

k_{v_i} is a positive control constant, f_d is a positive constant representing the desired grasping force magnitude at each contact and γ_s is an angle that is set by the designer in order to express the desired finger shaping. "Finger shaping" is in this work defined by the relative orientation of the two

fingers. Hereafter the following compact notation is used for an angle θ: $s_\theta \triangleq \sin\theta$ and $c_\theta \triangleq \cos\theta$.

The first term of (9) is introduced for joint damping. The second term represents applied forces of magnitude f_d at the direction of the line connecting the fingertips $\overrightarrow{t_1t_2} = \frac{\mathbf{p_{t_2}} - \mathbf{p_{t_1}}}{\|\mathbf{p_{t_2}} - \mathbf{p_{t_1}}\|}$ and the third term expresses the tangential contact forces at equilibrium as it will be clarified in the next section.

The proposed control law (9), (10) can be calculated using only the robotic finger forward kinematics and the radius of the hemispherical tips. Similarly to [23] and in contrast to [24], it does not require any knowledge of the tangential and normal directions at the contact and therefore no tactile sensing is needed. Similarly to [24] it optimizes the force angles at equilibrium as proved next and in contrast to [23] it does not require the use of on line estimates of tangential forces, neither conditions the grasping force magnitude on system parameters. Last but not least, in addition to what is achieved in [24] and [23], the proposed controller allows the choice of any finger shaping at equilibrium. Moreover γ_s may be time varying between an initial and a final shaping value in order to interactively transition from one finger shaping to another.

A. System Equilibrium

Substituting (9) into (7) utilizing (3) expanded by (4), (5), the closed loop system can be written in terms of the force errors as follows:

$$M_i\ddot{\mathbf{q}}_\mathbf{i} + C_{f_i}\dot{\mathbf{q}}_\mathbf{i} + D_{ii}{}^T\Delta f_i + A_{ii}{}^T\Delta\lambda_i + rJ_{\omega_i}{}^T\Delta N_i = 0 \quad (11)$$

$$M_o\ddot{\mathbf{p}}_\mathbf{o} - \sum_{i=1}^{2}(\mathbf{n_{c_i}}\Delta f_i + \mathbf{t_{c_i}}\Delta\lambda_i) = 0 \quad (12)$$

$$I_o\ddot{\theta}_o + \sum_{i=1}^{2}\hat{p}_{oc_i}^T(\mathbf{n_{c_i}}\Delta f_i + \mathbf{t_{c_i}}\Delta\lambda_i) + S_N = 0 \quad (13)$$

where

$$\Delta f_i = f_i - (-1)^{i+1}f_d\,\mathbf{n_{ci}}{}^T\frac{\mathbf{p_{t_2}} - \mathbf{p_{t_1}}}{\|\mathbf{p_{t_2}} - \mathbf{p_{t_1}}\|} \quad (14)$$

$$\Delta\lambda_i = \lambda_i - (-1)^{i+1}f_d\,\mathbf{t_{ci}}{}^T\frac{\mathbf{p_{t_2}} - \mathbf{p_{t_1}}}{\|\mathbf{p_{t_2}} - \mathbf{p_{t_1}}\|} \quad (15)$$

$$\Delta N_i = (-1)^{i+1}f_d\mathbf{t_{ci}}{}^T\frac{\mathbf{p_{t_2}} - \mathbf{p_{t_1}}}{\|\mathbf{p_{t_2}} - \mathbf{p_{t_1}}\|} - (-1)^{i+1}f_d s_\phi \quad (16)$$

$$S_N = \left(\hat{p}_{oc_1}^T - \hat{p}_{oc_2}^T\right)f_d\frac{\mathbf{p_{t_2}} - \mathbf{p_{t_1}}}{\|\mathbf{p_{t_2}} - \mathbf{p_{t_1}}\|} \quad (17)$$

and $C_{f_i} = (C_i + k_{v_i}I_3)$ with I_3 being the identity matrix of dimension 3.

Setting velocities and accelerations to zero in (11) yields $D_{ii}^T\Delta f_i + A_{ii}^T\Delta\lambda_i + J_{\omega_i}^T r\Delta N_i = 0$ which using (4), (5) can be written as $\begin{bmatrix}J_{v_i}^T & J_{\omega_i}^T\end{bmatrix}\begin{bmatrix}\mathbf{n_{ci}}\Delta f_i + \mathbf{t_{ci}}\Delta\lambda_i \\ r(\Delta\lambda_i + \Delta N_i)\end{bmatrix} = 0$. Assuming a full rank Jacobian matrix $J_i = \begin{bmatrix}J_{v_i}^T & J_{\omega_i}^T\end{bmatrix}$, we obtain $\mathbf{n_{ci}}\Delta f_i + \mathbf{t_{ci}}\Delta\lambda_i = 0$, $\Delta\lambda_i + \Delta N_i = 0$ that owing to the independent directions leads to:

$$\Delta f_i = \Delta\lambda_i = 0 \quad (18)$$

$$\Delta N_i = 0. \quad (19)$$

Notice that (18) satisfies the object's translational motion equation (12) at equilibrium. The physical meaning is that, at equilibrium, contact forces are at the direction of $\overrightarrow{t_1t_2}$ with magnitude $f_{c_i} = f_d$. Given (18), the object's rotational motion equation (13) yields $S_N = 0$ and in turn utilizing (17)

$$\left(\hat{p}_{oc_2}^T - \hat{p}_{oc_1}^T\right)\frac{\mathbf{p_{t_2}} - \mathbf{p_{t_1}}}{\|\mathbf{p_{t_2}} - \mathbf{p_{t_1}}\|} = 0 \quad (20)$$

Notice that $\mathbf{p_{oc_2}} - \mathbf{p_{oc_1}} = \mathbf{p_{c_2}} - \mathbf{p_{c_1}} \triangleq \overrightarrow{c_1c_2}$ is the interaction line vector; hence (20) indicates a zero outer product of $\overrightarrow{c_1c_2}$, $\overrightarrow{t_1t_2}$ which implies that these lines are parallel at equilibrium. Consequently, contact forces lie on the interaction line. Hence, force angles at equilibrium satisfy the following:

$$tan^{-1}\left(\frac{\lambda_i}{f_i}\right) = \phi_{fi} \quad (21)$$

To proceed, notice that if we express $\mathbf{p_{t_2}} - \mathbf{p_{t_1}}$ in frame $\{\delta\}$ denoted by left superscript we can write:

$$\begin{aligned}{}^\delta(\mathbf{p_{t_2}} - \mathbf{p_{t_1}}) &= {}^\delta(\mathbf{p_{c_2}} - r\mathbf{n_{c_2}}) - {}^\delta(\mathbf{p_{c_1}} - r\mathbf{n_{c_1}}) \\ &= R_{\delta L}[l\ 0]^T + rR_{c_1\delta}^T{}^{c_1}\mathbf{n_{c_1}} - rR_{c_2\delta}^T{}^{c_2}\mathbf{n_{c_2}} \\ &= \begin{bmatrix}l\,c_\alpha \\ l\,s_\alpha\end{bmatrix} + \begin{bmatrix}2rc_{\phi_0} \\ 0\end{bmatrix} \end{aligned} \quad (22)$$

where clearly ${}^{c_i}\mathbf{n_{c_i}} = [1\ 0]^T$ and respectively ${}^{c_i}\mathbf{t_{c_i}} = [0\ 1]^T$. Consequently,

$$\begin{aligned}\mathbf{n_{c_i}^T}(\mathbf{p_{t_2}} - \mathbf{p_{t_1}}) &= {}^{c_i}\mathbf{n_{c_i}^T}R_{c_i\delta}{}^\delta(\mathbf{p_{t_2}} - \mathbf{p_{t_1}}) \\ &= (-1)^{i+1}(lc_\alpha + 2rc_{\phi_0})c_{\phi_0} - ls_\alpha s_{\phi_0} \\ \mathbf{t_{c_i}^T}(\mathbf{p_{t_2}} - \mathbf{p_{t_1}}) &= {}^{c_i}\mathbf{t_{c_i}^T}R_{c_i\delta}{}^\delta(\mathbf{p_{t_2}} - \mathbf{p_{t_1}}) \\ &= (lc_\alpha + 2rc_{\phi_0})s_{\phi_0} + (-1)^{i+1}ls_\alpha c_{\phi_0}\end{aligned} \quad (23)$$

Utilizing (14), (15) yields, owing to (18), the values of f_i and λ_i at equilibrium. Substituting these equilibrium values in (21) leads to: $tan^{-1}\left(\frac{\mathbf{t_{c_i}}^T(\mathbf{p_{t_2}} - \mathbf{p_{t_1}})}{\mathbf{n_{c_i}}^T(\mathbf{p_{t_2}} - \mathbf{p_{t_1}})}\right) = \phi_{fi}$. Using (23) in the above expression and further substituting ϕ_{f_i} with respect to ϕ_0 and α from (1) yields $c_{\phi_0}s_\alpha = 0$. For opposing fingers, ϕ_0 remains within $(-\frac{\pi}{2}, \frac{\pi}{2})$ where $c_{\phi_0} \neq 0$. Hence, $s_\alpha = 0$ yields $\alpha = 0$ for $\alpha \in (-\frac{\pi}{2}, \frac{\pi}{2})$ indicating that the bisector of $2\phi_0$ is perpendicular to the interaction line at equilibrium.

Substituting $\alpha = 0$ in (22) we get the value of the length of fingertip line at equilibrium:

$$\|\mathbf{p_{t_2}} - \mathbf{p_{t_1}}\| = l + 2rc_{\phi_0} \quad (24)$$

Substituting $\alpha = 0$ and using (24) in (23) we get:

$$\mathbf{t_{c_i}}^T\frac{\mathbf{p_{t_2}} - \mathbf{p_{t_1}}}{\|\mathbf{p_{t_2}} - \mathbf{p_{t_1}}\|} = s_{\phi_0} \quad (25)$$

Hence, from (16) owing to (19) and using (25), it is proved that at equilibrium:

$$s_\phi = s_{\phi_0}. \quad (26)$$

It is now clear that $f_d s_\phi$ appearing in the third term of the controller (9) expresses tangential forces at equilibrium. In general (26) implies that, at equilibrium, $\phi = \pi - \phi_0$ or $\phi = \phi_0$ if $\phi \in (-\frac{\pi}{2}, \frac{\pi}{2})$. Substituting ϕ from (10) in the

latter yields

$$\phi_2 - \phi_1 = \phi_0 + \gamma_s \tag{27}$$

It is clear that γ_s affects the final relative finger orientation.

Summarizing the equilibrium state manifold of the closed loop system:

- Contact forces $[f_i \ \ \lambda_i]^T$ applied along $\overrightarrow{t_1 t_2}$ have a magnitude $f_{c_i} = f_d$
- Fingertip line $t_1 t_2$ is parallel to the interaction line $c_1 c_2$
- The bisector of $2\phi_0$ is perpendicular to the interaction line $c_1 c_2$ hence $\alpha = 0$ and $\phi_{fi} = \phi_0$ optimizing force angles
- The final relative finger orientation is: $\phi_2 - \phi_1 = \phi_0 + \gamma_s$.

B. Stability Analysis

To facilitate the analysis, we rewrite the closed loop system equation (7) - (9) in the following compact form collecting all Lagrange multipliers in the vector $\boldsymbol{\lambda} = [f_1 \ f_2 \ \lambda_1 \ \lambda_2]^T$ and all system position variables in $\mathbf{x} = [\mathbf{q_1}^T \ \mathbf{q_2}^T \ \mathbf{p_o}^T \ \theta_o]^T$.

$$M_s\ddot{\mathbf{x}} + C_s\dot{\mathbf{x}} + K_v\dot{\mathbf{x}} + A\boldsymbol{\lambda} - f_d \begin{bmatrix} {J_{v_1}}^T \frac{(\mathbf{p_{t_2}} - \mathbf{p_{t_1}})}{\|\mathbf{p_{t_2}} - \mathbf{p_{t_1}}\|} \\ -{J_{v_2}}^T \frac{(\mathbf{p_{t_2}} - \mathbf{p_{t_1}})}{\|\mathbf{p_{t_2}} - \mathbf{p_{t_1}}\|} \\ 0_{3\times 1} \end{bmatrix} - f_d \begin{bmatrix} {J_{\omega_1}}^T r s_\phi \\ -{J_{\omega_2}}^T r s_\phi \\ 0_{3\times 1} \end{bmatrix} = 0 \tag{28}$$

with

$$M_s = diag\,(M_1, M_2, M) \quad , \quad C_s = diag\,(C_1, C_2, 0_{3\times 3})$$
$$K_v = diag\,(k_{v_1} I_3, k_{v_2} I_3, 0_{3\times 3})$$
$$A = \begin{bmatrix} {D_{11}}^T & 0_{3\times 1} & {A_{11}}^T & 0_{3\times 1} \\ 0_{3\times 1} & {D_{22}}^T & 0_{3\times 1} & {A_{22}}^T \\ {D_{13}}^T & {D_{23}}^T & {A_{13}}^T & {A_{23}}^T \end{bmatrix} \tag{29}$$

Similarly, the constraints can be written compactly as: $A^T\dot{\mathbf{x}} = 0$.

Multiplying (28) by $\dot{\mathbf{x}}^T$ from the left assuming a constant γ_s yields: $\dfrac{dV}{dt} + W = 0$ where:

$$V = \frac{1}{2}\dot{\mathbf{x}}^T M_s \dot{\mathbf{x}} + f_d\|\mathbf{p_{t_1}} - \mathbf{p_{t_2}}\| + f_d r z\,(t) \tag{30}$$

$$W = k_{v_1}\|\dot{\mathbf{q}}_\mathbf{1}\|^2 + k_{v_2}\|\dot{\mathbf{q}}_\mathbf{2}\|^2 \tag{31}$$

where $z\,(t) = \int_0^\phi s_\xi \mathrm{d}\xi$. Clearly V is positive definite with respect to $\dot{\mathbf{x}}$, $\|\mathbf{p_{t_1}} - \mathbf{p_{t_2}}\|$ and $z\,(t)$ for $-\frac{\pi}{2} < \phi < \frac{\pi}{2}$ in the constraint manifold defined by $\mathcal{M}_c(\mathbf{x}) = \{\mathbf{x} \in \mathbb{R}^9 : A^T\dot{\mathbf{x}} = 0\}$. Given $\dot{V} = -W \leq 0$, it is clear that $V(t) \leq V\,(0)$ holds and consequently $\dot{\mathbf{x}}$, $\|\mathbf{p_{t_1}} - \mathbf{p_{t_2}}\|$ and $z\,(t)$ are bounded. From (16), (17) it can easily be concluded that ΔN_i and S_N are also bounded.

We write alternatively the closed loop system (11) - (13) in the following form utilizing (4) and (5):

$$M_s\ddot{\mathbf{x}} + C\dot{\mathbf{x}} + A\boldsymbol{\Delta\lambda} + B\boldsymbol{\Delta m} = 0 \tag{32}$$

$$C = C_s + K_v \quad , \quad B = \begin{bmatrix} r{J_{\omega_1}}^T & 0_{3\times 1} & 0_{3\times 1} \\ 0_{3\times 1} & r{J_{\omega_2}}^T & 0_{3\times 1} \\ 0_{3\times 1} & 0_{3\times 1} & [0\ 0\ 1]^T \end{bmatrix}$$

$$\boldsymbol{\Delta\lambda} = [\Delta f_1 \ \Delta f_2 \ \Delta\lambda_1 \ \Delta\lambda_2]^T \quad , \quad \boldsymbol{\Delta m} = [\Delta N_1 \ \Delta N_2 \ S_N]^T$$

In order to prove that $\boldsymbol{\Delta\lambda}$ is bounded, we multiply (32) by ${A^T M_s}^{-1}$ from the left, substituting $A^T\ddot{\mathbf{x}} = -\dot{A}^T\dot{\mathbf{x}}$ and multiplying again by $(A^T {M_s}^{-1} A)^{-1}$ we derive:

$$\boldsymbol{\Delta\lambda} = \left(A^T {M_s}^{-1} A\right)^{-1}\left(\dot{A}^T\dot{\mathbf{x}} - A^T {M_s}^{-1}\left(C\dot{\mathbf{x}} + B\boldsymbol{\Delta m}\right)\right)$$

Since ΔN_i, S_N are bounded, $\boldsymbol{\Delta m}$ is bounded and hence the term in the second parenthesis is bounded. Additionally, the matrix in the first parenthesis is bounded, thus $\boldsymbol{\Delta\lambda}$ is bounded. Hence from (32), $\ddot{\mathbf{x}}$ is also bounded and consequently $\dot{\mathbf{x}}$ is uniformly continuous. We may therefore deduce the convergence of $\dot{\mathbf{q}}_\mathbf{i}$ to zero while the contact and rolling constrains (3) yield that

$$\dot{\mathbf{p}}_\mathbf{o} - \hat{p}_{oci}\,\dot{\theta}_o \to 0 \tag{33}$$

Eliminating $\dot{\mathbf{p}}_\mathbf{o}$ by subtracting (33) (for $i = 1, 2$) yields: $(\hat{p}_{oc_2} - \hat{p}_{oc_1})\,\dot{\theta}_o \to 0$ and in turn $\dot{\theta}_o \to 0$ and from (33) $\dot{\mathbf{p}}_\mathbf{o} \to 0$. Hence, it is proved that system velocities converge to zero, $\dot{\mathbf{x}} \to 0$. Following the reasoning of Section III-A, we obtain $\Delta f_i, \Delta\lambda_i, \Delta N_i \to 0$. Since $\dot{\mathbf{x}}$ is bounded, $\mathbf{x}$ is uniformly continuous, therefore $\Delta\lambda$ and Δm are uniformly continuous from (14), (15). Consequently (32) leads to $\ddot{\mathbf{x}}$ being uniformly continuous, thus $\ddot{\mathbf{x}} \to 0$. Last from the rotational object equation (13), it is clear that $S_N \to 0$ and in turn following the reasoning of Section III-A $\alpha \to 0$ which implies that the force angles ϕ_{f_i} at equilibrium are optimal and equal to ϕ_0. Regarding $\mathbf{x}$ convergence it may be further proved following the proof line in [22] that $\dot{\mathbf{x}}$ converges to zero exponentially as $t \to \infty$.

Remark 1: If $\dot{\gamma}_s \neq 0$, (31) becomes $W' = k_{v_1}\|\dot{\mathbf{q}}_\mathbf{1}\|^2 + k_{v_2}\|\dot{\mathbf{q}}_\mathbf{2}\|^2 + \dot{\gamma}_s \sin\phi$. Considering $|\dot{\gamma}_s| \leq b$ for $b > 0$, W' can be bounded as follows: $W' \geq k_{v_1}\|\dot{\mathbf{q}}_\mathbf{1}\|^2 + k_{v_2}\|\dot{\mathbf{q}}_\mathbf{2}\|^2 - b$. Hence, it is easy to prove that $\dot{\mathbf{q}}_\mathbf{i}$, $i = 1, 2$ are uniformly ultimately bounded and will eventually go to zero since $\dot{\gamma}_s = 0$ at the final finger shaping value.

IV. SIMULATION RESULTS

We consider two identical robotic fingers, as depicted in Fig. 1, with $r = 0.01$ m and their parameters given in Table I. The fingers are positioned at distance $d = 0.02$ m and are initially at rest. We consider an object with a curved surface of semicircular shape with mass $m_o = 0.08$ Kg and $I_o = 6 \times 10^{-8}$. The initial system position is given in Table II and shown in Fig. 3 (blue line). The system is simulated under the proposed controller as well as the controllers of [24] and [23] for comparison purposes. Controller in [24] is given by:

$$\mathbf{u_i} = -k_{v_i}\dot{\mathbf{q}}_\mathbf{i} + f_d\big({D_{ii}}^T c_{\phi_0} + (-1)^{i+1}{A_{ii}}^T s_{\phi_0}\big)$$

while controller [23] is given by:

$$\mathbf{u_i} = -k_{v_i}\dot{\mathbf{q}}_\mathbf{i} + (-1)^i \frac{f_d}{2r} {J_{vi}}^T(\mathbf{p_{t_1}} - \mathbf{p_{t_2}}) - {J_{\omega_i}}^T r_i \hat{N}_i$$

where $\hat{N}_i = \frac{r_i}{\gamma_i}\int_0^t J_{\omega_i}\,\dot{\mathbf{q}}_\mathbf{i}\,\mathrm{d}\tau = \frac{r_i}{\gamma_i}\left(\phi_i(t) - \phi_i(0)\right)$ with γ_i being a positive constant estimator gain.

In all cases $k_{v_i} = 0.006$ for $i = 1, 2$ and $f_d = 4$ while $\gamma_i = 0.001$.

All three controllers achieve an equilibrium state shown in Fig. 3 - 5. Notice that the proposed controller keeps close to the initial finger shaping for $\gamma_s = 140^o$ (Fig. 3) similar to

Links	1	2	3
Masses (Kg)	0.045	0.03	0.015
Lengths (m)	0.04	0.03	0.02
Inertias (Kg m^2)			
$I_z \quad (\times 10^{-6})$	6	4	2

TABLE I: Robotic fingers parameters

Joints	$q_{i1}[deg]$	$q_{i2}[deg]$	$q_{i3}[deg]$
$i=1$	146.5335	-60.5216	-70
$i=2$	41.67	54	70
Object	$x_o[m]$	$y_o[m]$	$\theta_o[deg]$
	0.01752	0.055	0

TABLE II: Initial system pose

controllers [24] (Fig. 4) and [23] (Fig. 5). Keeping the initial finger shaping preserves grasp preshapes. It further achieves an equilibrium state with the smaller ϕ_0 as compared to the other two, although ϕ_0 minimization is not an explicit control objective. Notice that it is generally desirable to achieve an equilibrium state with small values of ϕ_0 because this is the final force angle and improves grasping in practice, keeping forces in the center of the friction cone.

Other desired finger shapings can be achieved for $\gamma_s = 0^o$ with $\phi_0 = -14.19^o$ and fingers almost parallel to each other and $\gamma_s = 90^o$ with $\phi_0 = -1.25^o$ and fingers almost perpendicular to each other (Fig. 6 and Fig. 7 respectively). The former shaping ($\gamma_s = 0^o$) is appropriate when powerful grasping forces are required (bulky object) as opposed to the latter ($\gamma_s = 90^o$) which is more suitable for delicate tip forces (thin object) [7]. Moreover, the former shaping may be more appropriate for a subsequent handover task while the latter is more suitable for a change of the object pose.

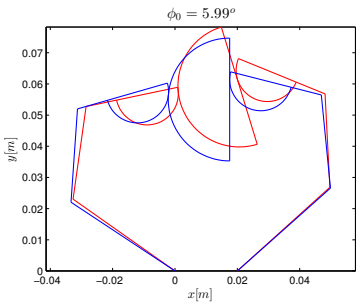

Fig. 3: Proposed control system for $\gamma_s = 140^o$

System time response for the case of $\gamma_s = 90^o$ are shown in Fig. 8 - Fig. 13 and are consistent with theoretical findings. Joint and object velocities as well as force errors converge to zero (Fig. 8, 9 and 10 respectively). Grasping force f_{c_i} (Fig. 11) is converging to the desired magnitude $f_d = 4\ N$ while force angles (Fig. 12) staying less than 20 degrees during grasping are converging to ϕ_0. The evolution of angles α, ϕ_0 and ϕ is shown in Fig. 13; as expected, angle α is converging to zero and ϕ to ϕ_0. Notice that for curved surfaced objects, ϕ_0 varies with contact location. In contrast, for polygonal shaped objects (eg. trapezoidal) ϕ_0 is constant, therefore γ_s precisely determines finger shaping through (27).

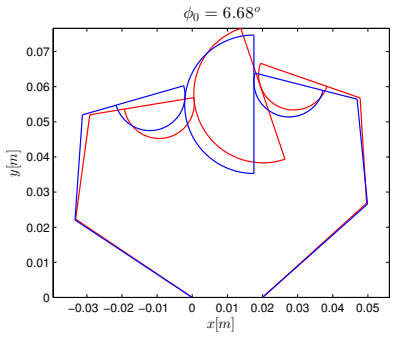

Fig. 4: Control system [24]

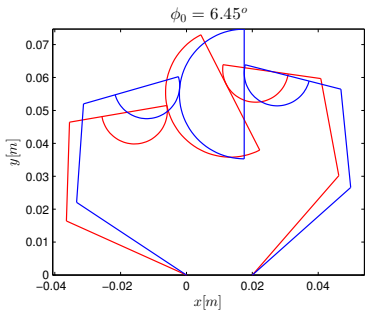

Fig. 5: Control system [23]

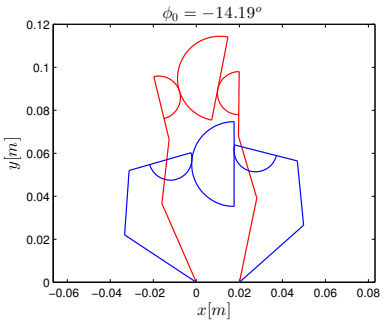

Fig. 6: Proposed control system for $\gamma_s = 0^o$

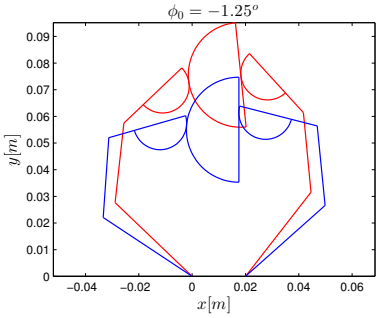

Fig. 7: Proposed control system for $\gamma_s = 90^o$

The proposed controller is not only able to achieve a stable

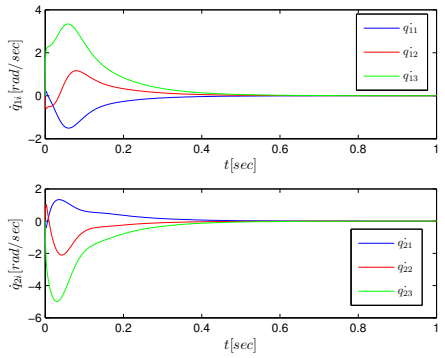

Fig. 8: Joint angular velocities

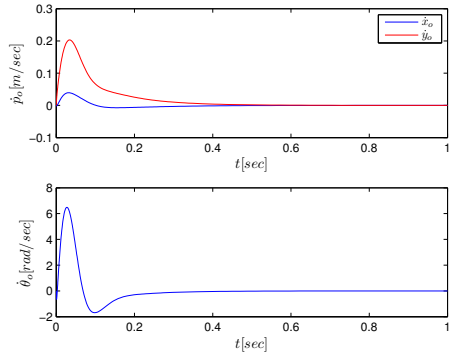

Fig. 9: Object translational and angular velocities

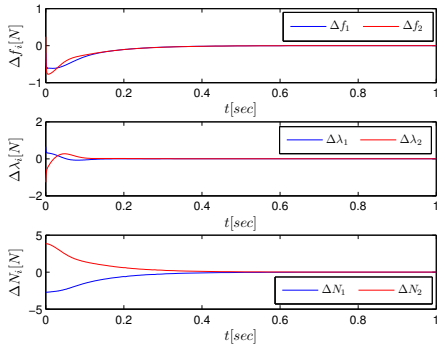

Fig. 10: Force error responses. (a) Normal force error Δf_i. (b) Tangential force error $\Delta\lambda_i$. (c) ΔN_i

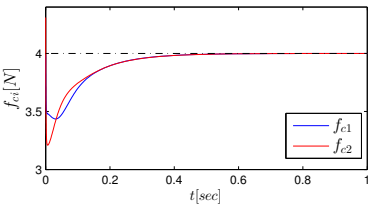

Fig. 11: Grasping force response

grasp without object sensing, with optimal force angle as well as with a desired finger shaping, but it also outperforms the other two controllers in many other aspects. First, con-

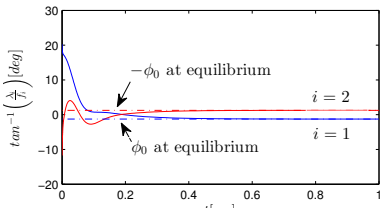

Fig. 12: Force angles

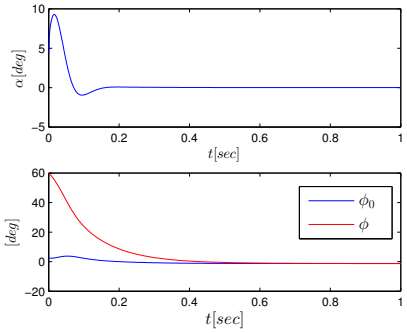

Fig. 13: Angles α, ϕ_0 and ϕ

troller [24] is very sensitive to contact direction measurement errors. We simulated the system with a divergence of 5^o and -5^o in $R_{c_i} = R(\phi_i + \phi_{t_i})$ for $i = 1, 2$ respectively, affecting $\mathbf{n_{c_i}}, \mathbf{t_{c_i}}$ involved in (4), (5). Simulation results show that system response is unstable as depicted in Fig. 14 - 15. Even smaller errors (1^o) lead the system to instability. The proposed controller does not require the knowledge of the contact normal and tangential directions. Second, controller [23] requires the use of an online estimate of the tangential forces which affects force transients that can become oscillatory depending on the choice of the estimator gain γ_i. Additionally, controller [23] achieves an equilibrium grasping force given by $f_{c_i} = \frac{f_d}{2r}(l + 2rc_{\phi_0})$; hence, it is dependent on system parameters that are varying for an arbitrary-shaped object (l, ϕ_0) thus being out of the control of the designer. Fig. 16 shows the grasping force response of the system with controller [23] which achieves an equilibrium value of 7.78 N instead of $f_d = 4$ N. This is a disadvantage particularly when grasping fragile objects. The proposed controller achieves a preset desired grasping force (Fig. 11) and therefore is safer when grasping such objects.

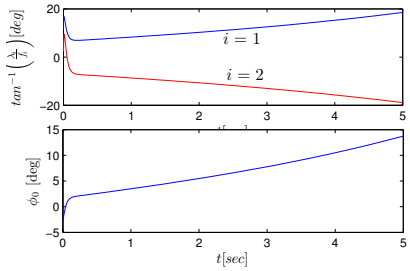

Fig. 14: Force angles and ϕ_0 evolution in case of contact direction error with controller [24]

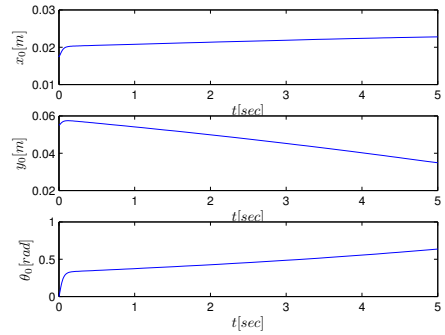

Fig. 15: Object position and orientation in case of contact direction error with controller [24]

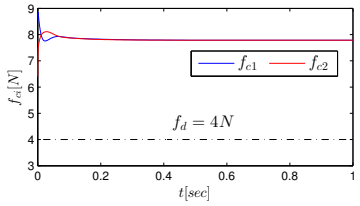

Fig. 16: Grasping force response with controller [23]

V. CONCLUSIONS

In this paper, a grasping controller for an arbitrary-shaped object is proposed which optimizes contact force angles without contact sensing while allowing any desired finger shaping. Grasp stability and force angle optimization is theoretically justified and validated via simulations. Comparison simulations showed that the proposed control law has significant advantages over two other grasping controllers which either become unstable in the presence of contact sensing measurement errors or they may break a fragile object at the sensorless case. Future work includes consideration of the gravity forces and extension to the three dimensional case.

REFERENCES

[1] A. Okamura, N. Smaby, and M. Cutkosky, "An overview of dexterous manipulation," in *IEEE International Conference on Robotics and Automation*, vol. 1, 2000, pp. 255–262.

[2] A. Bicchi, "Hands for dexterous manipulation and robust grasping: a difficult road toward simplicity," *IEEE Transactions on Robotics and Automation*, vol. 16, no. 6, pp. 652–662, 2000.

[3] T. Yoshikawa, "Multifingered robot hands: Control for grasping and manipulation," *Annual Reviews in Control*, vol. 34, no. 2, pp. 199–208, Dec. 2010.

[4] T. Wimbock, C. Ott, a. Albu-Schaffer, and G. Hirzinger, "Comparison of object-level grasp controllers for dynamic dexterous manipulation," *The International Journal of Robotics Research*, vol. 31, no. 1, pp. 3–23, Sept. 2011.

[5] M. T. Mason and J. K. Salisbury, *Robot Hands and the Mechanics of Manipulation*. Cambridge, MA: MIT Press, 1985.

[6] H. Kawasaki, T. Komatsu, and K. Uchiyama, "Dexterous anthropomorphic robot hand with distributed tactile sensor: Gifu hand ii," *IEEE/ASME Transactions on Mechatronics*, vol. 7, no. 3, pp. 296–303, Sept. 2002.

[7] K. Hoshino and I. Kawabuchi, "Pinching at fingertips for humanoid robot hand," *Journal of Robotics and Mechatronics*, vol. 17, no. 6, pp. 655–663, 2005.

[8] H. Liu, K. Wu, P. Meusel, N. Seitz, G. Hirzinger, M. Jin, Y. Liu, S. Fan, T. Lan, and Z. Chen, "Multisensory five-finger dexterous hand: The dlr/hit hand ii," in *IEEE/RSJ International Conference on Intelligent Robots and Systems*, Sept. 2008, pp. 3692–3697.

[9] SHADOW, "Shadow dexterous hand," 2010.

[10] R. Murray and S. Sastry, *A mathematical introduction to robotic manipulation*. CRC PressINC, 1994.

[11] C. Ferrari and J. Canny, "Planning optimal grasps," in *IEEE International Conference on Robotics and Automation*, 1992, pp. 2290–2295.

[12] C. Borst, M. Fischer, and G. Hirzinger, "Grasp planning: how to choose a suitable task wrench space," in *IEEE International Conference on Robotics and Automation,*, 2004, pp. 319–325.

[13] J. Chen and M. Zribi, "Control of multifingered robot hands with rolling and sliding contacts," *International Journal of Advanced Manufacturing Technology*, vol. 16, no. 1, pp. 71–77, Jan. 2000.

[14] A. Cole, P. Hsu, and S. Sastry, "Dynamic control of sliding by robot hands for regrasping," *IEEE Transactions on Robotics and Automation*, vol. 8, no. 1, pp. 42–52, 1992.

[15] R. Nakashima and T. Yoshikawa, "On dynamic control of finger sliding and object motion in manipulation with multifingered hands," *IEEE Transactions on Robotics and Automation*, vol. 16, no. 5, pp. 469–481, 2000.

[16] S. Arimoto, P. T. A. Nguyen, H.-y. Han, and Z. Doulgeri, "Dynamics and control of a set of dual fingers with soft tips," *Robotica*, vol. 18, no. 1, pp. 71–80, 2000.

[17] Z. Doulgeri, J. Fasoulas, and S. Arimoto, "Feedback control for object manipulation by a pair of soft tip fingers," *Robotica*, vol. 20, no. 1, pp. 1–11, Jan. 2002.

[18] S. Arimoto, K. Tahara, M. Yamaguchi, P. Nguyen, and M.-Y. Han, "Principles of superposition for controlling pinch motions by means of robot fingers with soft tips," *Robotica*, vol. 19, no. 01, pp. 21–28, Jan. 2001.

[19] S. Arimoto, K. Tahara, J.-H. Bae, and M. Yoshida, "A stability theory of a manifold: concurrent realization of grasp and orientation control of an object by a pair of robot fingers," *Robotica*, vol. 21, no. 02, pp. 163–178, Feb. 2003.

[20] S. Arimoto, *Control Theory of Multi-fingered Hands: A Modelling and Analytical-mechanics Approach for Dexterity and Intelligence*. Springer-Verlag London Limited, 2008.

[21] R. Ozawa, S. Arimoto, and S. Nakamura, "Control of an object with parallel surfaces by a pair of finger robots without object sensing," *IEEE Transactions on Robotics*, vol. 21, no. 5, pp. 965–976, Oct. 2005.

[22] S. Arimoto, "A differential-geometric approach for 2d and 3d object grasping and manipulation," *Annual Reviews in Control*, vol. 31, no. 2, pp. 189 – 209, 2007.

[23] M. Yoshida, S. Arimoto, and K. Tahara, "Pinching 2d object with arbitrary shape by two robot fingers under rolling constraints," in *IEEE/RSJ International Conference on Intelligent Robots and Systems*, 2009, pp. 1805–1810.

[24] S. K. Song, J. B. Park, and Y. H. Choi, "Dual-fingered stable grasping control for an optimal force angle," *IEEE Transactions on Robotics*, vol. 28, no. 1, pp. 256–262, 2012.

[25] R. Ozawa and S. Arimoto, "Multi-fingered dynamic blind grasping with tactile feedback in a horizontal plane," in *IEEE International Conference on Robotics and Automation*, 2006, pp. 1006–1011.

[26] M. Prats, P. J. Sanz, and A. P. Pobil, "A framework for compliant physical interaction," *Autonomous Robots*, vol. 28, no. 1, pp. 89–111, Sept. 2009.